Transition Metal Chemistry (2020) 45:139–145
https://doi.org/10.1007/s11243-019-00366-8

Insight into molecular packing effects on transesterification catalysis of zinc(II) coordination polymers

Lingling Yang[1] · Dongwon Kim[1] · Soomin Hyun[1] · Young-A Lee[2] · Ok-Sang Jung[1]

Received: 19 October 2019 / Accepted: 20 November 2019 / Published online: 7 December 2019

Abstract
Self-assembly of ZnX_2 ($X^- = ClO_4^-$ and $CF_3SO_3^-$) with naphthalene-2,6-diyl-diisonicotinate (L) gives rise to the 2D sheet structures with composition of $[ZnL_2(H_2O)_2](ClO_4)_2{\cdot}H_2O$ and $[ZnL_2(CF_3SO_3)_2]$, respectively. $[ZnL_2(H_2O)_2](ClO_4)_2{\cdot}H_2O$ is packed in an interpenetration mode, whereas $[ZnL_2(CF_3SO_3)_2]$ exists as a simple 2D network in the crystalline solid state. These two crystals have been employed as hetero-catalysts for transesterification reactions of phenylacetate with alcohol. The catalytic effect on the transesterification reaction shows the order of $[ZnL_2(H_2O)_2](ClO_4)_2{\cdot}H_2O > Zn(CF_3SO_3)_2 > [ZnL_2(OTf)_2] > Zn(ClO_4)_2$, which indicate that molecular packing is an important factor in the catalysis.

Introduction

Construction of desirable coordination architectures including their spatial arrangement is a far-reaching issue and, not coincidentally, resulting in a great advance of task-specific molecular functions [1–7] such as molecular separation, small molecular adsorption, molecular containers, ion exchangers, chemo-recognition, and hetero-catalysis [7–14]. In particular, their catalytic efficiencies have been highly dependent on solvent systems, molecular dimensions, solubility, local geometry around metal centers, counteranions, etc. [15–19]. Among various organic reactions, transesterification reaction is of an important mission in the field of mass production of polyesters, glycerols, and biodiesels in both academic and industrial laboratories [20–22]. Thus, some zinc(II) coordination compounds have been extensively examined for appropriate Lewis acidity and homogeneous catalysis of the transesterification reactions [23, 24]. Such transesterification reactions using zinc(II) complexes could be affected by various factors: halides bound to Zn(II) ion, discrete and infinite structures [17, 25], and trace water in the reaction system.

To our knowledge, this research presents a landmark transesterification catalysis effect on the space arrangement of 2D zinc(II) coordination polymers. In this context, we herein report the results on structural properties of 2D Zn(II) coordination polymers along with their heterogeneous catalysis for the transesterification reaction of phenyl acetate with methanol.

Experimental

Materials and physical measurements

All chemicals including zinc(II) perchlorate, zinc(II) trifluoromethanesulfonate, 3-bromopyridine, 2,6-dihydroxynaphthalene, triethylamine, and phenyl acetate were purchased from Sigma-Aldrich, and were used without further purification. Elemental microanalyses (C, H, N) were performed on crystalline samples at the KBSI Pusan Center using a Vario-EL III analyzer. Infrared spectra were obtained on a Nicolet 380 FT-IR spectrophotometer using samples prepared as KBr pellets. ^{1}H (300 MHz) spectra were recorded on a Varian Mercury Plus 300. Thermal analyses were performed under N_2 at a scan rate of 10 °C/min using a PerkinElmer-TGA-DSC 4000.

Electronic supplementary material The online version of this article (https://doi.org/10.1007/s11243-019-00366-8) contains supplementary material, which is available to authorized users.

✉ Ok-Sang Jung
oksjung@pusan.ac.kr

[1] Department of Chemistry and Research Institute of Functional Materials Chemistry, Pusan National University, Pusan 609-735, Korea

[2] Department of Chemistry, Chonbuk National University, Jeonju 54896, Korea

Preparation of naphthalene-2,6-diyl-diisonicotinate (L)

Triethylamine (6.40 mL, 50 mmol) in chloroform (10 mL) was slowly added to a mixture of 2,6-dihydroxynaphthalene (1.60 g, 10 mmol) and isonicotinoyl chloride (3.92 g, 22 mmol) in chloroform (120 mL). The reaction mixture was refluxed for 12 h. The solution was washed with distilled water several times. The chloroform layer was dried over $MgSO_4$ and filtered. Evaporation of the chloroform solvent gave white solid. Yield: 87%. m.p. 246 °C. Anal. Calcd for $C_{22}H_{14}N_2O_4$ (%): C, 71.35; H, 3.81; N, 7.56. Found: C, 72.10; H, 3.98; N, 7.51. IR (KBr, cm^{-1}): 1739 (vs), 1608 (w), 1560 (w), 1513 (w), 1411 (w), 1324 (w), 1274 (vs), 1207 (s), 1143 (s), 1128 (w), 1091 (w), 1064 (w), 939 (w), 900 (w), 752 (m), 700 (m), 640 (w). ^{1}H NMR ($CDCl_3$, 300 MHz, δ): 8.90 (d, $^3J = 5.28$ Hz, 4H), 8.07 (d, $^3J = 5.28$ Hz, 4H), 7.94 (d, $^3J = 8.80$ Hz, 3H), 7.77 (s, 2H), 7.42 (d, 2H). ^{13}C NMR ($CDCl_3$, 75 MHz, δ): 163.91, 150.91, 148.26, 136.66, 131.96, 129.52, 123.26, 121.80, 118.73.

Preparation of $[ZnL_2(H_2O)_2](ClO_4)_2{\cdot}H_2O$

A chloroform solution (5 mL) of L (3.7 mg, 0.01 mmol) was carefully layered onto a water/acetone solution (4.5 mL of acetone and 0.5 mL of H_2O) of zinc(II) perchlorate (3.7 mg, 0.01 mmol). After 4 days, transparent crystals suitable for X-ray single crystallography were obtained in a 56% yield. m.p. 297 °C. Anal. Calcd for $C_{44}H_{34}Cl_2N_4O_{24}Zn$ (%): C, 46.40; H, 3.01; N, 4.92. Found: C, 46.57; H, 3.18; N, 5.03. IR (KBr pellet, cm^{-1}): 1739(s), 1560(w), 1508(w), 1419(w), 1272(vs), 1207(m), 1145(s), 1120(vs), 1087(s), 1062(w), 904(w), 808(w), 752(w), 636(w), 482(w).

Preparation of $[ZnL_2(CF_3SO_3)_2]$

A tetrahydrofuran solution (3.0 mL) of L (3.7 mg, 0.01 mmol) was carefully layered onto a tetrahydrofuran solution (3.0 mL) of zinc(II) trifluoromethanesulfonate (3.6 mg, 0.01 mmol). After 3 days, colorless crystals suitable for X-ray single crystallography were obtained in a 60% yield. m.p. 330 °C. Anal. Calcd for $C_{46}H_{28}F_6N_4O_{14}S_2Zn$ (%): C, 50.03; H, 2.56; N, 5.07. Found: C, 50.43; H, 2.82; N, 5.03. IR (KBr pellet, cm^{-1}): 1743(s), 1619(w), 1560(w), 1511(w), 1419(w), 1276(vs), 1205(s), 1130(m), 1089(w), 1060(w), 1035(m), 902(w), 848(w), 752(w), 646(m), 480(w).

Transesterification catalysis

In order to scrutinize the transesterification catalytic effects of the 2D coordination polymers, $[ZnL_2(H_2O)_2](ClO_4)_2{\cdot}H_2O$, $[ZnL_2(CF_3SO_3)_2]$, $Zn(ClO_4)_2$, and $Zn(CF_3SO_3)_2$ have been employed as a catalyst of the transesterification reaction of phenyl acetate with methanol. In the present research, the transesterification of phenyl acetate (68 mg, 0.5 mmol) at 50 °C with an excess amount of methanol was accomplished. For instance, phenyl acetate (68 mg, 0.5 mmol) and each catalyst (32–33 mg, 0.03 mmol) were stirred in methanol (5 ml), and warmed up to 50 °C. The catalytic process was monitored by reference to the ^{1}H NMR spectra.

X-ray single crystallography

All X-ray crystallographic data were collected on a Bruker SMART automatic diffractometer with a graphite-monochromated Mo Kα radiation ($\lambda = 0.71073$ Å) and a CCD detector at − 25 °C. The thirty-six frames of two-dimensional diffraction images were collected and processed to obtain the cell parameters and orientation matrix. Data integration and reduction were undertaken with SAINT and XPREP [26]. Absorption effects were corrected by the multi-scan method using SADABS [27]. The structures were solved by the direct method and refined by full-matrix least squares techniques (SHELXL 2014/07) [28, 29]. The non-hydrogen atoms were refined anisotropically, and hydrogen atoms were placed in calculated positions and refined using a riding model. The crystal parameters and procedural information corresponding to the data collection and structure refinement are listed in Table 1.

Results and discussion

Synthetic aspects

The new ligand, naphthalene-2,6-diyl-diisonicotinate (L), was synthesized by the reaction of 2,6-dihydroxynaphthalene with isonicotinoyl chloride according to the literature method [30]. Self-assembly of ZnX_2 ($X^- = ClO_4^-$ and $CF_3SO_3^-$) with L produced transparent crystals consisting of 2D coordination frameworks as shown in Scheme 1. The 2D structure of $[ZnL_2(CF_3SO_3)_2]$ was simply packed, whereas that of $[ZnL_2(H_2O)_2](ClO_4)_2{\cdot}H_2O$ was packed in an interpenetration mode in the crystalline state. The self-assembly reaction was initially carried out in the 1:2 mol ratio of ZnX_2/L, but the reaction was not so significant to the formation of the 2D networks. The crystalline products are quite stable under the aerobic condition, and are insoluble in water and general organic solvents such as acetone, chloroform, acetonitrile, and dissociated in strong polar solvents such as dimethyl sulfoxide and *N,N*-dimethylformamide. The compositions and structures were confirmed by elemental analyses, IR, thermal analysis (Figs. S1–S5), and single crystal X-ray diffraction. The characteristic strong IR band

Table 1 Crystal data and structural refinements for and $[ZnL_2(H_2O)_2](ClO_4)_2{\cdot}H_2O$ and $[Zn(CF_3SO_3)_2L_2]$

	$[ZnL_2(H_2O)_2](ClO_4)_2{\cdot}H_2O$	$[Zn(CF_3SO_3)_2L_2]$
Formula	$C_{44}H_{36}Cl_2N_4O_{24}Zn$	$C_{46}H_{28}F_6N_4O_{14}S_2Zn$
M_w (g mol^{-1})	1141.04	1104.21
Cryst. system	Orthorhombic	Tetragonal
Space group	Cmca	$P4_32_12$
a (Å)	21.4841 (3)	21.7072 (3)
b (Å)	11.7590 (2)	21.7072 (3)
c (Å)	17.9849 (2)	12.5426 (2)
α (°)	90	90
β (°)	90	90
γ (°)	90	90
V (Å^3)	4543.55 (11)	5910.11 (19)
Z	4	4
ρ (g cm^{-3})	1.668	1.241
μ (mm^{-1})	0.757	0.563
$F(000)$	2336	2240
R_{int}	0.0309	0.0743
GoF on F^2	1.165	1.043
R_1 [I > 2σ(I)][a]	0.0613	0.0431
wR_2 (all data)[b]	0.1855	0.1072
Completeness (%)	100% (θ = 25.242°)	100% (θ = 25.242°)

[a] $R_1 = \Sigma||F_o| - |F_c||/\Sigma|F_o|$

[b] $wR_2 = (\Sigma[w(F_o^2 - F_c^2)^2]/\Sigma[w(F_o^2)^2])^{1/2}$

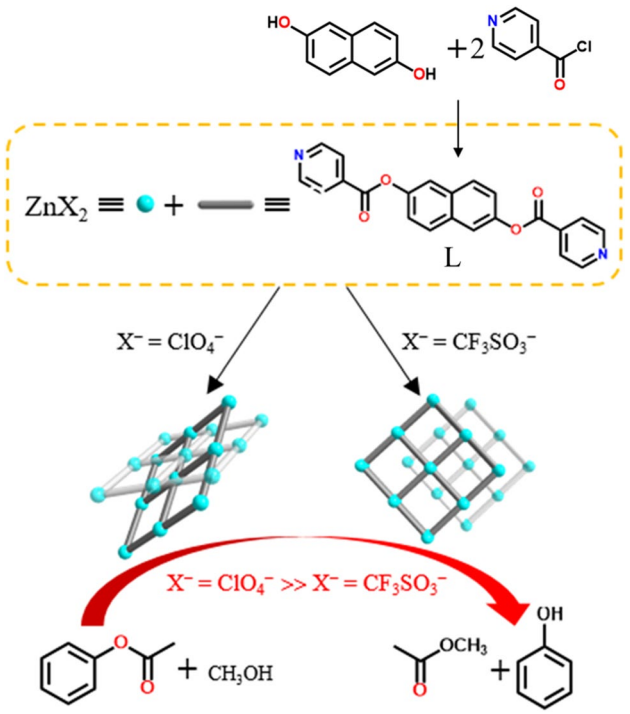

Scheme 1 Synthetic procedure and catalytic effects

at 1087 cm^{-1} of $[ZnL_2(H_2O)_2](ClO_4)_2{\cdot}H_2O$ and 1276 cm^{-1} of $[ZnL_2(CF_3SO_3)_2]$ was found to correspond to ClO_4^- and $CF_3SO_3^-$, respectively.

X-ray crystal structures

The crystal structures are shown in Fig. 1, and their relevant bond lengths and angles are listed in Table 2. For $[ZnL_2(H_2O)_2](ClO_4)_2{\cdot}H_2O$, the local geometry of the zinc(II) ion is an octahedral arrangement with two water molecules in transposition (O–Zn–O = 180.0°) and four pyridine units in propeller fashion building the basal plane. Each linker ligand connects two zinc(II) ions defining 2D network with the edges of a $[Zn(II)]_4$ rhombus unit (Zn···Zn = 37.843 Å; Zn···Zn = 21.484 Å; 76-membered ring). The most interesting feature is that the crystal structures show the occurrence of the 2D interpenetrated packing (dihedral angle = 36.21°) in the solid state (Fig. S9). The ClO_4^- anion exists as a simple counteranion (Zn···O = 4.617 Å), and instead water molecules are coordinated to the central Zn(II) ion in a transposition (Zn–O = 2.160(3) Å). Solvate water molecule is positioned in a long distance (Zn···O = 4.165 Å). For $[ZnL_2(CF_3SO_3)_2]$, the ligand acts as a spacer between two octahedral zinc(II) ions with four pyridine moieties defining a 2D network with the edges of a [Zn(II)] square (Zn···Zn = 30.699 Å; Zn···Zn = 30.699 Å; 76-membered ring). The $CF_3SO_3^-$ anions exist as a coordination mode (Zn-OSO_2CF_3 = 2.191(3) Å) in transposition rather than counteranions. Inner disordered tetrahydrofuran was squeezed. In the $[ZnL_2(CF_3SO_3)_2]$ case, the guest accessible void volumes were calculated as 31.0% (1833.2/5910.1 Å^3) for all crystals, removed electrons (474e$^-$/8 ≒ 60e$^-$) were calculated by PLATON [29]. The 2D network of $[ZnL_2(CF_3SO_3)_2]$ has a simple packing, consisting of *abab*… layers instead of such an interwoven structure. Thus, their packing motifs are quite different owing in part to the metallophilicity of anions (Fig. 2).

Transesterification catalysis

In order to scrutinize the packing and counteranion effects of the present 2D coordination polymers on transesterification catalysis, the coordination polymers were employed as heterogeneous catalysts for the reaction of phenyl acetate with methanol. To date, many useful catalysts for transesterifications under mild reaction conditions have been developed [25, 31]. $[ZnL_2(H_2O)_2](ClO_4)_2{\cdot}H_2O$ (0.05 mmol) showed a significant catalytic effect on the transesterification of phenyl acetate (0.5 mmol) at 50 °C with an excess amount of methanol (Fig. 3 and Table 3). The catalysis was monitored by reference to the ^{1}H NMR spectra (Fig. S4). The catalysis finished within 45 h, whereas the catalysis using $[ZnL_2(CF_3SO_3)_2]$ proceeded by only 48% for 45 h. Such a

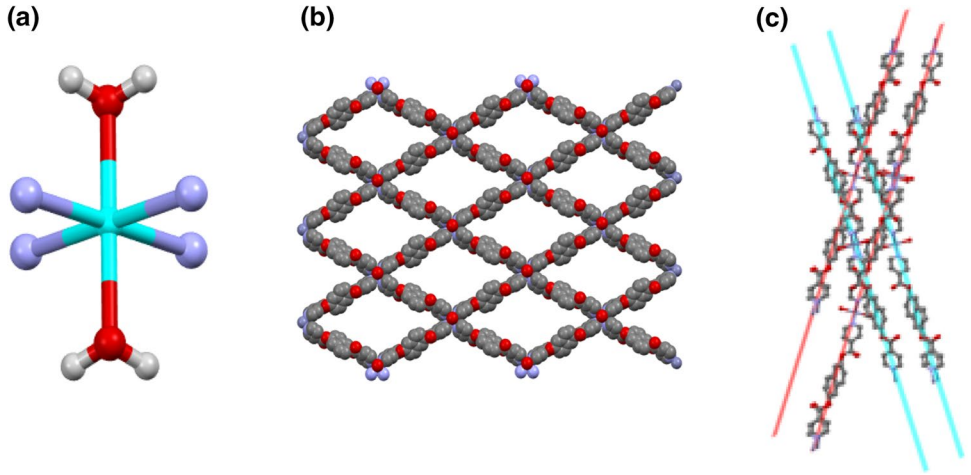

Fig. 1 Perspective view of octahedral coordination geometry around Zn(II) sites of $[Zn(CF_3SO_3)_2L_2]$ (**a**), crystal packing in the space-filling mode (**b**), and packing in an interpenetration mode (**c**)

Table 2 Selected bond lengths (Å) and angles (°) $[ZnL_2(H_2O)_2](ClO_4)_2{\cdot}H_2O$ and $[Zn(CF_3SO_3)_2L_2]$

$[ZnL_2(H_2O)_2](ClO_4)_2{\cdot}H_2O$		$[Zn(CF_3SO_3)_2L_2]$	
Zn(1)–O(8)	2.160 (3)	Zn(1)–N(2)$^{\#1}$	2.132 (3)
Zn(1)–O(8)$^{\#1}$	2.160 (3)	Zn(1)–N(2)	2.132 (3)
Zn(1)–N(1)	2.185 (3)	Zn(1)–N(1)$^{\#2}$	2.160 (3)
Zn(1)–N(1)$^{\#1}$	2.185 (3)	Zn(1)–N(1)$^{\#3}$	2.160 (3)
Zn(1)–N(1)$^{\#2}$	2.185 (3)	Zn(1)–O(7)	2.191 (3)
Zn(1)–N(1)$^{\#3}$	2.185 (3)	Zn(1)–O(7)$^{\#1}$	2.191 (3)
O(8)–Zn(1)–O(8)$^{\#1}$	180.0	N(2)$^{\#1}$–Zn(1)–N(2)	91.7 (2)
O(8)–Zn(1)–N(1)	90.71 (9)	N(2)$^{\#1}$–Zn(1)–N(1)$^{\#2}$	176.5 (1)
O(8)$^{\#1}$–Zn(1)–N(1)	89.29 (9)	N(2)–Zn(1)–N(1)$^{\#2}$	90.8 (1)
O(8)–Zn(1)–N(1)$^{\#1}$	89.29 (9)	N(2)$^{\#1}$–Zn(1)–N(1)$^{\#3}$	90.8 (1)
O(8)$^{\#1}$–Zn(1)–N(1)$^{\#1}$	90.71 (9)	N(2)–Zn(1)–N(1)$^{\#3}$	176.5 (1)
N(1)–Zn(1)–N(1)$^{\#1}$	180.0 (1)	N(1)$^{\#2}$–Zn(1)–N(1)$^{\#3}$	86.8 (2)
O(8)–Zn(1)–N(1)$^{\#2}$	89.3 (9)	N(2)$^{\#1}$–Zn(1)–O(7)	91.2 (1)
O(8)$^{\#1}$–Zn(1)–N(1)$^{\#2}$	90.7 (9)	N(2)–Zn(1)–O(7)	87.1 (1)
N(1)–Zn(1)–N(1)$^{\#2}$	89.8 (1)	N(1)$^{\#2}$–Zn(1)–O(7)	86.5 (1)
N(1)$^{\#1}$–Zn(1)–N(1)$^{\#2}$	90.2 (1)	N(1)$^{\#3}$–Zn(1)–O(7)	95.3 (1)
O(8)–Zn(1)–N(1)$^{\#3}$	90.7 (9)	N(2)$^{\#1}$–Zn(1)–O(7)$^{\#1}$	87.1 (1)
O(8)$^{\#1}$–Zn(1)–N(1)$^{\#3}$	89.3 (9)	N(2)–Zn(1)–O(7)$^{\#1}$	91.2 (1)
N(1)–Zn(1)–N(1)$^{\#3}$	90.2 (1)	N(1)$^{\#2}$–Zn(1)–O(7)$^{\#1}$	95.3 (1)
N(1)$^{\#1}$–Zn(1)–N(1)$^{\#3}$	89.8 (1)	N(1)$^{\#3}$–Zn(1)–O(7)$^{\#1}$	86.5 (1)
N(1)$^{\#2}$–Zn(1)–N(1)$^{\#3}$	180.0	O(7)–Zn(1)–O(7)$^{\#1}$	177.5 (2)
$^{\#1}-x+1, -y-1, -z-1$; $^{\#2}$ $x, -y-1, -z-1$; $^{\#3}-x+1, y, z$		$^{\#1}$ $-y, -x, -z+1/2$; $^{\#2}$ $-y+1, -x, -z+1/2$; $^{\#3}$ $x, y-1, z$	

different catalytic activity can be explained by the difference in packing, counteranion, or coordination environment. The catalytic reaction using $[ZnL_2(H_2O)_2](ClO_4)_2{\cdot}H_2O$, moreover, is more effective than that of several heterogeneous Brønsted-acid solids such as porous zeolites [32], acid-leached natural kaolinite [33], sulfated SnO_2 [34], and trimetallic zinc(II) complexes [25]. Furthermore, the control catalytic reactions using authentic $Zn(ClO_4)_2$ and $Zn(CF_3SO_3)_2$ salts were attempted in this research. The catalyses using $Zn(ClO_4)_2$ and $Zn(CF_3SO_3)_2$ exhibited a reverse trend relative to $[ZnL_2(H_2O)_2](ClO_4)_2{\cdot}H_2O$ and $[ZnL_2(CF_3SO_3)_2]$, indicating that the counteranion is not so significant in the catalytic reaction. Thus, the catalytic effect on the transesterification reaction shows the order of $[ZnL_2(H_2O)_2](ClO_4)_2{\cdot}H_2O > Zn(CF_3SO_3)_2 > Zn(ClO_4)_2 > [Zn(CF_3SO_3)_2L_2]$. In particular, $[ZnL_2(H_2O)_2](ClO_4)_2{\cdot}H_2O$ efficiently survives after catalysis, and thus $[ZnL_2(H_2O)_2](ClO_4)_2{\cdot}H_2O$ was found to be a good recyclable heterogeneous catalyst (Fig. 4). The recyclable catalysis showed 85% activity. The catalytic effects of L (Fig. S5) and the same

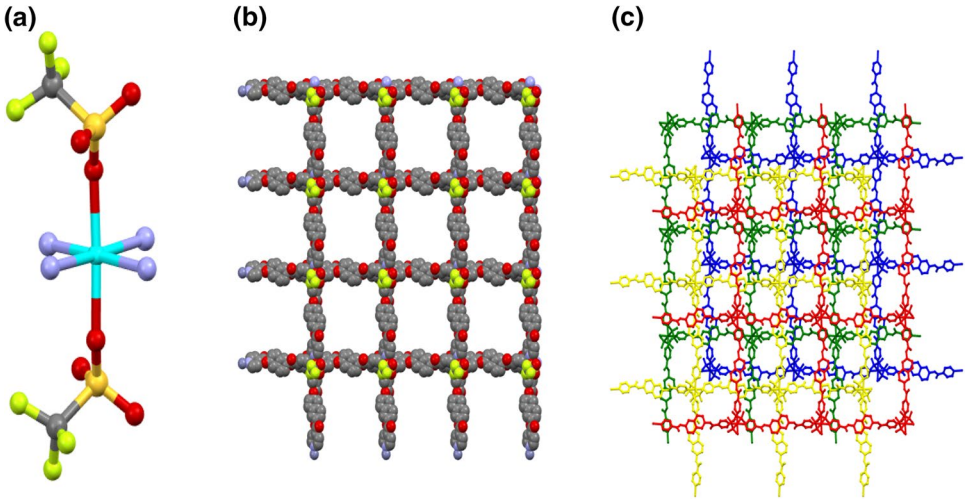

Fig. 2 Perspective view of octahedral coordination geometry around Zn(II) sites of $[ZnL_2(H_2O)_2](ClO_4)_2{\cdot}H_2O$ (**a**), crystal packing in the space-filling mode (**b**), and packing in a simple mode (**c**)

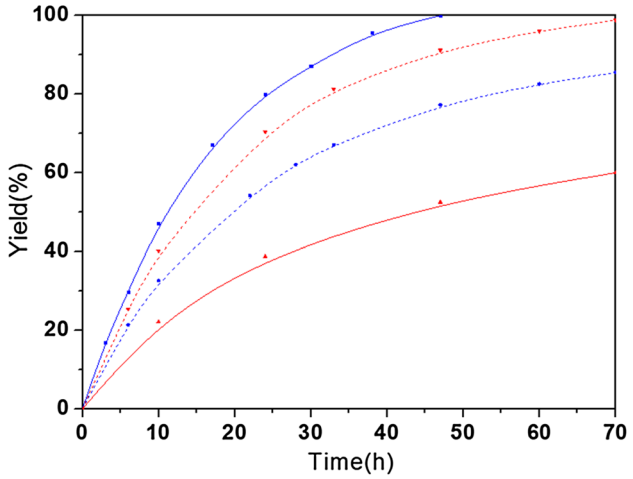

Fig. 3 Plot showing transesterification catalysis % conversions of phenyl acetate with methanol using $[ZnL_2(H_2O)_2](ClO_4)_2{\cdot}H_2O$ (solid blue line), $Zn(ClO_4)_2$ (dotted blue line), $[Zn(CF_3SO_3)_2L_2]$ (solid red line), $Zn(CF_3SO_3)_2$ (dotted red line) at 50 °C. (Color figure online)

reaction in the presence of trace water (Fig. S6) were also studied for comparison. The catalysis with trace water, as expected, proceeded slowly. The mechanism of heterogeneous-zinc(II)-ion-catalyzed transesterification probably involves electrophilic activation of the carbonyl moiety, specifically by binding of the zinc(II) to the carbonyl oxygen [31]. Thus, the vacant sites and the Lewis acidity of the zinc(II) center, accordingly, play important roles in the transesterification catalytic reactions. The significant heterogeneous catalytic activity can be explained by the density of Zn(II) ions and the stability of the 2D interpenetrated coordination polymers relative to general simple 2D coordination polymers. It seems that the catalytic effects, as plotted for the present case, are strongly dependent on the packing mode. For the reaction system, ethanolysis is much slower than methanolysis; for example, ethanolysis reaches to 20% after 80 h at 50 °C, 100% 80 h at 70 °C in (Fig. S7).

Table 3 Transesterification catalysis reaction conditions and % conversions

Catalysis solvents	Catalysts	Temp. (°C)	Time (h)	% Conversion
MeOH	L	50	70	41
	$[ZnL_2(H_2O)_2](ClO_4)_2{\cdot}H_2O$		50	100
	$[Zn(CF_3SO_3)_2L_2]$		70	58
	$Zn(ClO_4)_2$		70	100
	$Zn(CF_3SO_3)_2$		70	85
MeOH + H_2O (4: 0.1)	$[ZnL_2(H_2O)_2](ClO_4)_2{\cdot}H_2O$	50	70	52
	$[Zn(CF_3SO_3)_2L_2]$			40
	$Zn(CF_3SO_3)_2$ + L			19
EtOH	$Zn(ClO_4)_2$ + L	50	95	28
	$Zn(CF_3SO_3)_2$ + L		95	26
	$[ZnL_2(H_2O)_2](ClO_4)_2{\cdot}H_2O$		95	24
Propanol	$[ZnL_2(H_2O)_2](ClO_4)_2{\cdot}H_2O$	50	95	8
		70	80	100

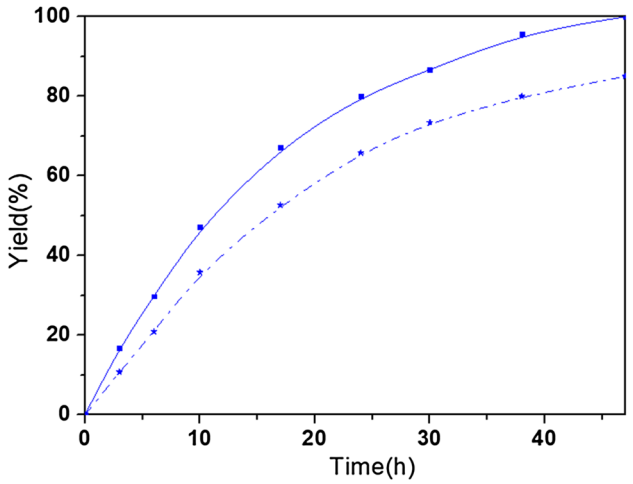

Fig. 4 Plot showing catalytic % conversions of transesterification of phenyl acetate with methanol using $[ZnL_2(H_2O)_2](ClO_4)_2{\cdot}H_2O$ (solid blue line = first run; dashed blue line = second recycled crystals) in methanol at 50 °C. (Color figure online)

Conclusion

Self-assembly of ZnX_2 ($X^- = ClO_4^-$ and $CF_3SO_3^-$) with a new ligand L produced colorless single crystals consisting of 2D coordination polymers with the same topology, but their packing structure is different, the simple 2D and interpenetrated 2D packing structure. The 2D network crystals have been used in the heterogeneous catalysis of phenyl acetate with methanol, indicating that the particular 2D packing mode is an important factor in the transesterification catalysis reaction. This result clearly shows what we believe to be the first study into molecular packing effects of catalysts on the general heterogenous transesterification catalytic reaction. More systematic studies, for example on the synthesis of related ligands, are in progress. Further experiments on the packing structure will provide more detailed structural information on the catalytic effects of the coordination polymers.

Supplementary data

IR spectra, ^{1}H NMR spectra, and TGA curves of $[ZnL_2(H_2O)_2](ClO_4)_2{\cdot}H_2O$, $[ZnL_2(CF_3SO_3)_2]$ were available in Supplementary material. Crystallographic data for the structure reported here have been deposited with the Cambridge Crystallographic Data Centre (Deposition No. CCDC 1892785-1892786 for $[ZnL_2(H_2O)_2](ClO_4)_2{\cdot}H_2O$, $[ZnL_2(CF_3SO_3)_2]$.), respectively. These data can be obtained free of charge from the Cambridge Crystallographic Data Centre via www.ccdc.cam.ac.uk/data_request/cif.

Acknowledgements This work was supported by National Research Foundation of Korea (NRF) grants funded by the Korean Government [MEST] (2016R1A2B3009532 [OSJ], 2016R1A5A1009405 [OSJ] and 2017R1D1A3B03035719) (YAL).

References

1. Schoedel A, Li M, Li D, O'Keeffe M, Yaghi OM (2016) Chem Rev 116:12466
2. Moon SY, Kim E, Noh TH, Lee YA, Jung OS (2013) Dalton Trans 42:13974
3. Chen L, Chen Q, Wu M, Jiang F, Hong M (2015) Acc Chem Res 48:201
4. Mellot-Draznieks C, Dutour J, Ferey G (2004) Angew Chem Int Ed Engl 43:6290
5. Jiang J, Zhao Y, Yaghi OM (2016) J Am Chem Soc 138:3255
6. Hyde ST, O'Keeffe M, Proserpio DM (2008) Angew Chem Int Ed Engl 47:7996
7. Ahmad N, Chughtai AH, Younus HA, Verpoort F (2014) Coord Chem Rev 280:1
8. Noori Y, Akhbari K (2017) RSC Adv 7:1782
9. Weng CH, Cheng SC, Wei HM, Wei HH, Lee CJ (2006) Inorg Chim Acta 359:2029
10. Ahmed I, Jhung SH (2014) Mater Today 17:136
11. Lin KS, Adhikari AK, Ku CN, Chiang CL, Kuo H (2012) Int J Hydrog Energy 37:13865
12. Leenders SH, Gramage-Doria R, Bruin B, Reek JN (2015) Chem Soc Rev 44:433
13. Dyson PJ, Jessop PG (2016) Catal Sci Technol 6:3302
14. Murase T, Nishijima Y, Fujita M (2012) J Am Chem Soc 134:162
15. Park M, Kim H, Lee H, Noh TH, Jung OS (2014) Cryst Growth Des 14:4461
16. Rolff M, Schottenheim J, Decker H, Tuczek F (2011) Chem Soc Rev 40:4077
17. Kim H, Park M, Lee H, Jung OS (2015) Dalton Trans 44:8198
18. Saitoh M, Balch AL, Yuasa J, Kawai T (2010) Inorg Chem 49:7129
19. Solomon EI, Heppner DE, Johnston EM, Ginsbach JW, Cirera J, Qayyum M, Kieber-Emmons MT, Kjaergaard CH, Hadt RG, Tian L (2014) Chem Rev 114:3659
20. Meyer JL, Bakir M, Lan P, Economy J, Jasiuk I, Bonhomme G, Polycarpou AA (2019) Macromol Mater Eng 304:1800647
21. Ana GL, Daniel V, Diego EB, Pedro Y, Jesus E (2018) Fermentation 4:75
22. Jung JM, Oh JL, Kwon D, Park YK, Zhang M, Lee J, Kwon EE (2019) Energy Convers Manag 195:1
23. Thirunavukkarasu K, Sankaranarayanan TM, Pandurangan A, Shanthi RV, Sivasanker S (2014) Catal Sci Technol 4:851
24. Niu X, Wang F, Li X, Zhang R, Wu Q, Sun P (2019) Ind Eng Chem Res 58:5698
25. Lee H, Noh TH, Jung OS (2014) Dalton Trans 43:3842
26. Nonius B (2013) APES SAINT and XPREP Bruker AXS INC
27. Shin JW, Eom K, Moon D (2016) J Synchrotron Radiat 23:369
28. Sheldrick GM (2014) SHELXL-2014/7: a Program for Structure Refinement. University of Göttingen, Göttingen
29. Spek AL (2003) PLATON: a multipurpose crystallographic tool. Utrecht University, Utrecht
30. Cho Y, Kim JG, Noh TH, Jung OS (2013) J Mol Struct 1047:95
31. Felices LS, Escudero-Adàn EC, Benet-Buchholz J, Kleij AW (2009) Inorg Chem 48:846
32. Balaji BS, Sasidharan M, Kumar R, Chanda B (1996) Chem Commun 6:707

33. Ponde DE, Deshpande VH, Bulbule VJ, Sudalai A, Gajare AS (1998) J Org Chem 63:1058
34. Chavan SP, Zubaidha PK, Dantale SW, Keshavaraja A, Ramaswamy AV, Ravindranathan T (1996) Tetrahedron Lett 37:233